Desalination and Water Treatment
www.deswater.com
doi: 10.1080/19443994.2015.1048305

57 (2016) 11945–11955
June

Taylor & Francis
Taylor & Francis Group

Vacuum enhanced direct contact membrane distillation for oil field produced water desalination: specific energy consumption and energy efficiency

Khaled Okiel[a], Abdel Hameed M. El-Aassar[b], Tarek Temraz[c], Salah El-Etriby[c], Hosam A. Shawky[b,*]

[a]*Gemsa Petroleum Company, New El-maadi, Cairo, Egypt, Tel. +20 1002553048; email: khaledmazher@yahoo.com*
[b]*Egyptian Desalination Research Center of Excellence EDRC, Desert Research Center, El-Matariya, P.O.B. 11753, Cairo, Egypt, Tel. +20 1002501524; email: hameed_m50@yahoo.com (A.H.M. El-Aassar), Tel. +20 1002930710; Fax: +20 226389069; email: hashawky@EDRC.gov.eg (H.A. Shawky)*
[c]*Faculty of Science, Suez Canal University, Ismailia, Egypt, Tel. +20 1148866440; email: ttemraz@yahoo.com (T. Temraz), Tel. +20 1001545863; email: s_eletreby@yahoo.com (S. El-Etriby)*

Received 6 September 2014; Accepted 26 April 2015

ABSTRACT

This paper presents a study for energy requirements of lab-scale membrane distillation (MD) unit. This lab unit consists of flat-sheet membrane module with two circulation pumps, heater, and cooler to study the effect of different operating conditions on both specific energy consumption (SEC) and energy efficiency (η_E) via vacuum enhanced direct contact MD method. The flux and the two parameters of energy (SEC, η_E) were measured using different temperatures, different feed flow rates, and different feed salt concentrations. The two membranes used were neat polypropylene (PP) membrane and PP/multi-walled carbon nanotubes (MWCNTs) composite membrane. The membranes were synthesized via phase inversion process, using xylene as a solvent, methyl iso-butyl ketone as a coagulant and dispersion medium for MWCNTs. The results showed that the highest η_E was 39.5 with SEC 1,649.2 kW h/m^3 at flux 52.5 kg/m^2 h using 15 L/min feed flow rate of synthetic feed water with salt concentration 10,000 ppm at 55°C feed temperature. On the other hand, using our prepared membrane for the desalination of oil field water, the values of η_E and SEC were 12.1 and 4,189.5 kW h/m^3, respectively.

Keywords: Direct contact membrane distillation; Oil field produced water; Specific energy consumption; Energy efficiency

1. Introduction

Membrane distillation (MD) is a novel process that can be adapted effectively for water desalination or water treatment in industrial applications [1,2]. MD refers to a thermally driven transport of vapor through non-wetted porous hydrophobic membranes, the driving force being the vapor pressure difference between the two sides of the membrane pores. Hot-side temperatures under 90°C are suitable; hence, this process is ideal for exploiting waste heat or solar thermal resources. However, a number of issues, remain before this technology, are fully deployed commercially.

There are different MD configurations such as (i) direct contact membrane distillation, (ii) sweeping gas

*Corresponding author.

membrane distillation, (iii) vacuum membrane distillation, and (iv) air gap membrane distillation that can be used for various applications (desalination, environmental/waste cleanup, water-reuse, food, medical, etc.). MD is an energy intensive process, it has advantages such as: a nearly complete rejection of non-volatile components, a low operating pressure that is not related to feed concentration as is the case for reverse osmosis (RO), a small vapor space, and low operating temperatures (40–80˚C) applicable in dewatering thermally sensitive solutions [3,4].

The performance of membrane distillation mainly depends on the membrane properties, the operating conditions, and the module design [5,6].

Direct contact membrane distillation (DCMD) is the simplest MD configuration, and is widely employed in desalination of seawater and brackish waters, in DCMD the hot solution (feed) is in direct contact with the hot membrane side surface. Therefore, evaporation takes place at the feed membrane surface. The vapor is moved by the pressure difference across the membrane to the permeate side and condenses inside the membrane module. Because of the hydrophobic characteristic, the feed cannot penetrate the membrane (only the gas phase exists inside the membrane pores) [7–10].

The performance of DCMD can be improved in different ways. High temperature DCMD (e.g. DCMD with the same temperature difference, but at higher temperatures) can achieve higher water fluxes than low-temperature DCMD [11]. This is because vapor pressure increases exponentially with increasing water temperature. In another configuration, vacuum-enhanced DCMD (VEDCMD), the cooler water stream flows under negative pressure (vacuum). Under specific operating conditions, VEDCMD has been shown to increase the flux by up to 85% when compared to the conventional DCMD configuration [11–13].

For MD process, the porous hydrophobic membrane acts as a barrier layer. It prevents the penetration of the aqueous solution into its dry pores by its hydrophobicity nature until the liquid entry pressure of water is exceeded [14]. The membrane properties include pore size, pore size distribution, membrane thickness, and porosity [15–17]. Therefore, good hydrophobicity, appropriate pore size, and narrow pore size distribution of microporous membranes are necessary to ensure the high permeate flux and rejection in MD process.

The previous works [18,19] found that the increase in the flow rate and feed temperature caused an increase in the MD process efficiency. If high fluxes are targeted, both membrane and module characteristics must be adequate. The good characteristics of only one of them (module or membrane) will not produce the desired flux because its good characteristics can be overshadowed by inadequate behavior of the other one [20]. Nowadays, poly-tetra-fluoro-ethylene, polypropylene (PP) and poly-vinylidene-fluoride are the most popular and available hydrophobic membrane materials that give high performance especially after improvement using different nanomaterials [1,2].

Energy analysis in thermal distillation such as multistage flash distillation and membrane desalination processes RO are well studied; however, only a little information is available on energy analysis for MD process [21]. To estimate the energy efficiency (η_E) of MD process, the concept of gained output ratio (GOR) is the ratio of the latent heat of evaporation of the produced water to the total input energy in the MD system [22]. The GOR reflects how well the energy input in the system is utilized for the water production. The higher the GOR value, better is the performance of the system. In thermal desalination process, the GOR is an important parameter whereas a good multi-effect distillation system may have a GOR of 12 [23].

The energy consumption in MD systems includes both thermal energy necessary to heat the feed aqueous solution and to cool the permeate aqueous solution, or condensation and the electrical energy required to run the circulation pumps [1]. To date, the studies reported in literature on membrane distillation mainly investigate the temperature polarization phenomena, heat efficiency/heat transfer and only few studies refer to the energy requirements. Concerning this point, several authors propose the internal heat recovery as a way to reduce the external heat supply for DCMD [22,24,25]. One of the interesting parameters for a desalination plant is the specific energy consumption (SEC), which is defined as the energy input required to produce 1 m^3 of distillate (i.e. ratio of energy supplied to the volume of produced fresh water). Also, it is more adequate to use energy efficiency (η_E) to characterize an MD system instead of the thermal efficiency, since energy efficiency (η_E) takes into consideration the global energy input, which includes both thermal energy and electrical energy [22].

The present work is concerned with the calculation of both SEC and energy efficiency (η_E) in VEDCMD system. Detailed investigations have been conducted to understand the relationships between the water flux/production and operation parameters, including feed temperature, feed and permeate velocities, feed concentration. Moreover, this study examined the variation of the SEC and energy efficiency (η_E) with the operation parameters. Also, the study investigates the effect of different parameters that consume energy for the desalination process of brine oil field produced water. The experiments were achieved using both neat and improved polypropylene (PP, PP/multi-walled carbon nanotubes (MWCNTs)) membranes at different feed temperatures, feed flow rates, and salt concentrations.

2. Experimental part and methodology

2.1. The VEDCMD unit

The VEDCMD unit setup is schematically depicted in Fig. 1. The membrane cell consisted of two compartments, the feed side and the permeate side [11–13]. The compartments were made of polyacrylic to resist corrosion by NaCl solution. The module was positioned horizontally so that the feed solution flowed through the bottom compartment of the cell while the cooling water passed through the upper compartment. The feed and permeate were separated by the hydrophobic porous membrane. The effective area of the membrane was 0.0018 m^2. A cooler for the regulation of the cold stream temperature (0.55 kW); a thermostatic bath for the regulation of the hot stream temperature (1.5 kW); two flow meters for the regulation of the flow rate of the two streams; two pumps (the cold pump 135 W and the hot pump 300 W); two manometers for registering the module inlet pressures of the two streams; four thermocouples (accuracy ±0.1˚C) for evaluating the module inlet and outlet temperatures of both streams. The volume tank of the hot stream was of 15 L, the volume tank of hot stream was 10 L. The feed and cold solutions were contained in double-walled reservoirs and circulated through the membrane module using centrifugal pumps. The outlet temperatures of the hot and cold sides were continually monitored and recorded. The permeated liquid was circulated through a graduated cylinder, and the volume was measured at regular intervals. The salinity of

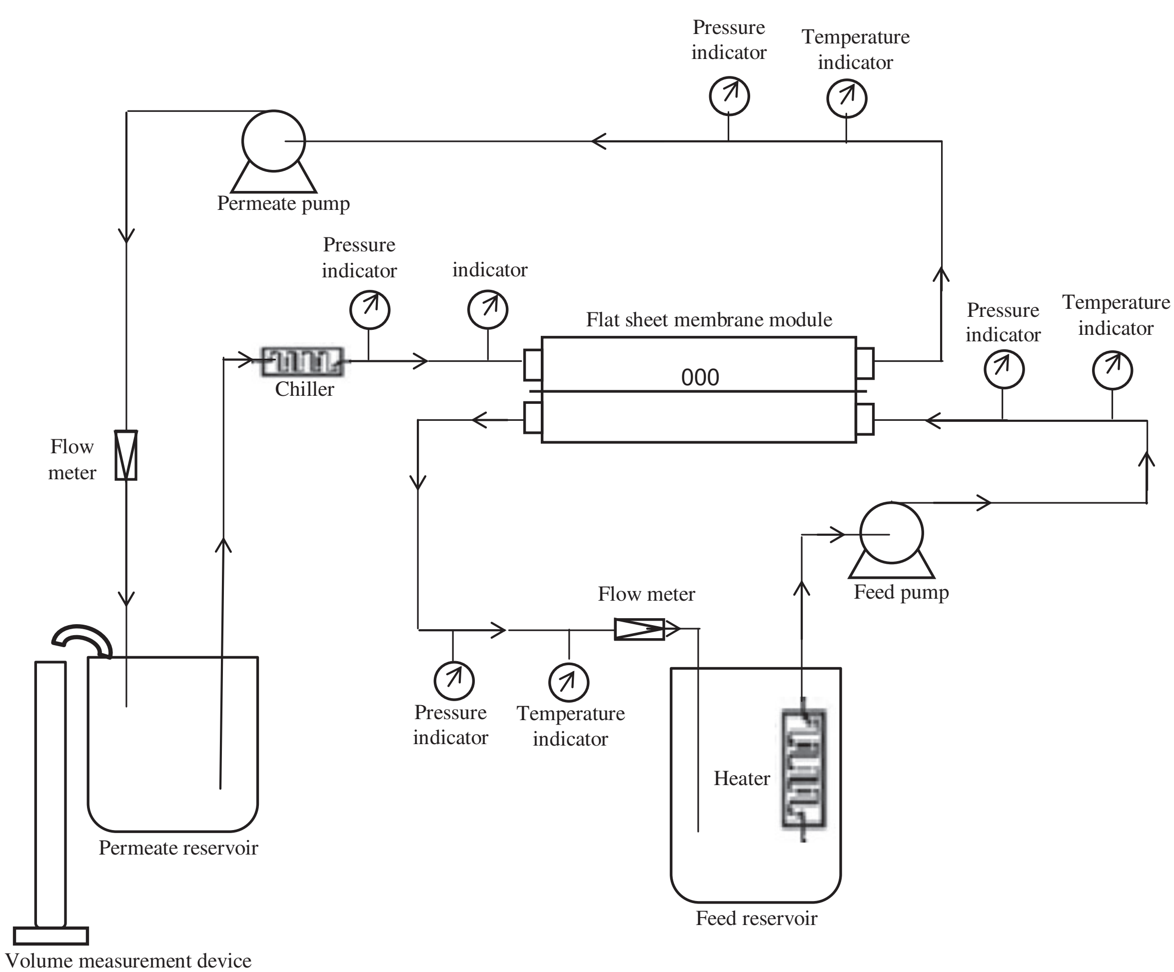

Fig. 1. VEDCMD experimental setup [11–13].

the feed water was determined through water conductivity using an electrical conductivity meter (EC470-L, ISTEK, Korea), and it should be noted here that any increase in permeate conductivity indicated that liquid water passed through the membrane so that the result was rejected, in other words the salt rejection was 99.99%.

In order to check the presence of leakages in the system, as well as the membrane hydrophobicity, the volume in the graduated cylinder was observed when only the hot stream was recirculated for at least 30 min before starting the experiment. Each experiment was, then, initiated only when no variation was reported on the display for the time of observation. During the experiments, the feed was at atmospheric pressure and its flow rate varied between 6 and 15 L/min. The feed temperature varied between 40 and 60˚C. In all tests, the distillate flow rate was kept at about 6 L/min and the distillate temperature was in the range of 13–14˚C with negative pressure (−3 psi), where the cold centrifugal pump was installed to drown the cold stream as shown in Fig. 1.

2.2. Membranes type

Two types of prepared membranes were used in this work. The first membrane was neat PP, and the second was improved PP/MWCNTs with 5 mg/g (CNT/polymer concentration). The membranes were prepared via phase inversion method. The casting solution was prepared by dissolving a specific weight of PP using xylene as a solvent. The casting solution was heated to around 130˚C with stirring at 320 rpm until PP was completely dissolved and a clear solution was obtained. Then, the polymer solution was cast over heated glass plate at 118˚C. The cast films were exposed to solvent evaporation for a predetermined time of 60 min. The solvent was allowed to evaporate until a gel membrane was obtained. Detailed membrane preparation procedures were presented in our previous work [26].

The improved PP membranes with MWCNTs, MWCNTs were placed in 10 mL methyl isobutyl ketone, which used as a dispersion medium, with continuous stirring at 450 rpm for 24 h. After that, the casting solution of PP was added with continuous stirring. Membrane was then obtained by casting the PP solution on a glass plate in an oven at 118˚C.

The resulting membranes were immersed in hot water (at 80˚C) for three hours to remove any excessive solvent. The obtained membranes were stored in distilled water for the measurements of membrane characterization and performance experiments. The pore size and thickness of the used membranes are given in Table 1.

2.3. Feed water samples

The synthetic feed water used in this work was a distilled water containing different concentrations of NaCl salt and the permeate water was distilled water.

The oil field produced wastewater samples with total dissolved salts (TDS) 230,000 mg/L from Gemsa petroleum company—oil treatment facilities—located in eastern desert in Egypt were collected from the main effluent wastewater pipeline after wastewater treatment unit before disposal. The general characteristics of produced water were carried out in the Egyptian Petroleum Research Institute, analysis and evaluation department, central laboratory, and the results of crude oil and produced water are given in Table 2.

2.4. Methodology for energy calculation

Energy consumption in DCMD system includes the thermal energy necessary to heat up the feed aqueous solution to be treated and to cool down the permeate aqueous solution, and the electrical energy required to run the circulation pumps [22]:

$$E_{\mathrm{in}}\ (\mathrm{W}) = E_{\mathrm{t}} + E_{\mathrm{e}} \tag{1}$$

where E_{in} is the total energy consumed in membrane distillation, (E_{t}) is the thermal energy necessary to heat up the feed aqueous solution to be treated and to cool down the permeate aqueous solution in watt, and (E_{e}) is the electrical energy required to run the circulation pumps in watt.

2.4.1. Electrical energy required to run the circulation pumps [27]

The power to pump water can be expressed as:

$$E_{\mathrm{pump}}\ (\mathrm{W}) = 9797\, Q\, H\, g \tag{2}$$

Table 1
Thickness and pore size of the used membrane

No.	Membrane type	Pore size (nm)	Thickness (μm)
1	Polypropylene	453	50
2	(PP/MWCNTs)	846	50

Table 2
Chemical composition of wastewater (after wastewater treatment plant treatment)

Constituents	mg/L
Total dissolved solids	231,985
Conductivity	21.2×10^{-2} mohs/cm @ 22.5℃
Density	1.15819 g/mL @ 60 F
Oil in water	5.0

Q is the flow rate in cubic meters per second and H is the pump head in meters (pressure in meters of water), g is the specific gravity in SI units ($g = 1$).

$$E_e = E_{\text{heating site pump}} + E_{\text{cooling site pump}} \tag{3}$$

2.4.2. Thermal energy consumption for heating or cooling [22,24]

The thermal energy consumptions were calculated considering the heating and cooling of hot and cold stream, where the equations used for obtaining the heating and cooling energy are reported below:

$$q_h = \dot{m}_f C_{p,f}(T_{f,in} - T_{f,out}) \tag{4}$$

$$q_c = \dot{m}_p C_{p,p}(T_{p,in} - T_{p,out}) \tag{5}$$

where q_h, q_c are the heating and cooling energy (W), respectively, $\dot{m}_p$ is the feed mass flow rate (kg/s), $\dot{m}_p$ is the permeate mass flow rate (kg/s), $C_{p,f}$ is the heat capacity of feed water in J/kg K, $C_{p,p}$ is the heat capacity of permeate water in J/kg K, $T_{f,in}$, $T_{p,in}$ are the feed and distillate temperature at module inlet (K), and $T_{f,out}$, $T_{p,out}$ are the feed and distillate temperature at module outlet.

$$E_t = q_h + q_c \tag{6}$$

SEC (kWh/m^3) is defined as [22] the energy input required to produce 1 m^3 of distillate (i.e. ratio of energy supplied to the volume of produced fresh water).

$$\text{SEC} = \frac{E_{in}(\text{kW})}{V_{dis.}\left(\frac{\text{m}^3}{\text{h}}\right)} \tag{7}$$

where $V_{dis.}$ is the volume (in m^3) of water gained in 1 h.

2.5. Energy efficiency calculations [5,22]

Energy efficiency (η_E) is defined as the as the ratio between effective heat for evaporation to the total input energy.

$$\eta_E = \frac{\text{Effective heat for evaporation}}{\text{Total energy input}} \tag{8}$$

$$\eta_E = \frac{J\ A\ \Delta \boldsymbol{H}_v}{E_t + E_e} \tag{9}$$

where J is the water flux in m^3/m^2 s, A is the membrane area in m^2, and $\Delta \boldsymbol{H}_v$ is the latent heat of vaporization of water in J/kg.

It should be noted here that the change of water properties due to temperature change and TDS change was taken into account using the polynomial equations used [28,29].

3. Results and discussion

3.1. The effect of operating conditions on flux

3.1.1. The effect of feed temperature on flux

Fig. 2 shows the effect of feed temperature on the permeation flux for both membranes. The experiments were carried out using different feed temperature ranging from 45 to 60℃ at hot flow rate 12 L/min, with feed TDS of 10,000 ppm. As depicted, an increase in temperature increases the permeation flux. This is completely in agreement with the previous reported results [8,16,18]. MWCNTs/PP nanocomposite membrane showed better performance when compared to that of neat PP membrane. Also, Fig. 2 shows that MWCNTs/PP nanocomposite membrane possesses better flux when compared with neat PP membrane at the same feed temperatures. At 60℃, the maximum flux achieved was (55.3 L/m^2 h) for MWCNTs/PP nanocomposite membrane when compared with (39.4 L/m^2 h) for neat PP membrane.

3.1.2. The effect of feed flow rate on flux

Feed flow rate can directly affect the permeation flux by decreasing the temperature and concentration polarization effects, or in better description by reducing the effect of temperature and concentration boundary layers [7,8]. In this study, feed flow rate values of 6, 10, 12, and 15 L/min were tested as the second operating variable at feed temperature 55℃, feed TDS 10,000 ppm. Generally, the permeation flux increases by increasing the feed flow rate at both membranes

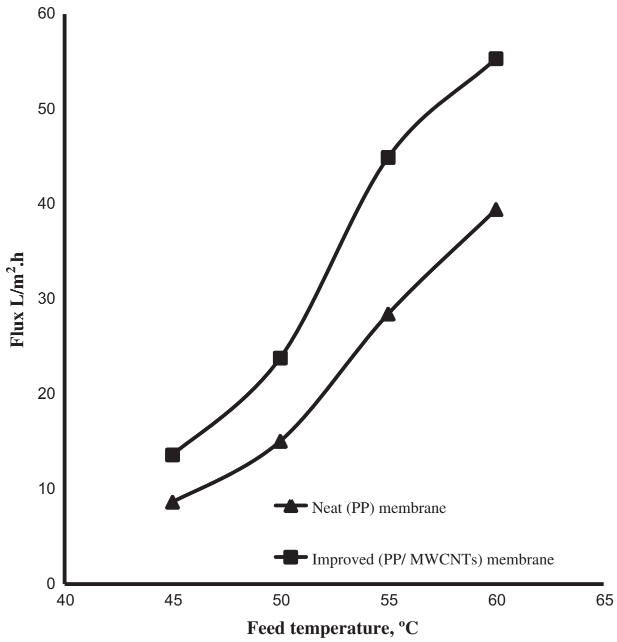

Fig. 2. Effect of feed temperature on water flux.

(Fig. 3). MWCNTs /PP nanocomposite membrane showed better performance when compared to neat PP membrane resulted in an increase in the flow rate from 6 to 15 L/min led to increase in the permeation flux. More flux was found in MWCNTs /PP nanocomposite membrane (52.5 L/m^2 h) rather than 34.5 L/m^2 h in the neat PP membrane at feed flow rate 15 L/min (Fig. 3).

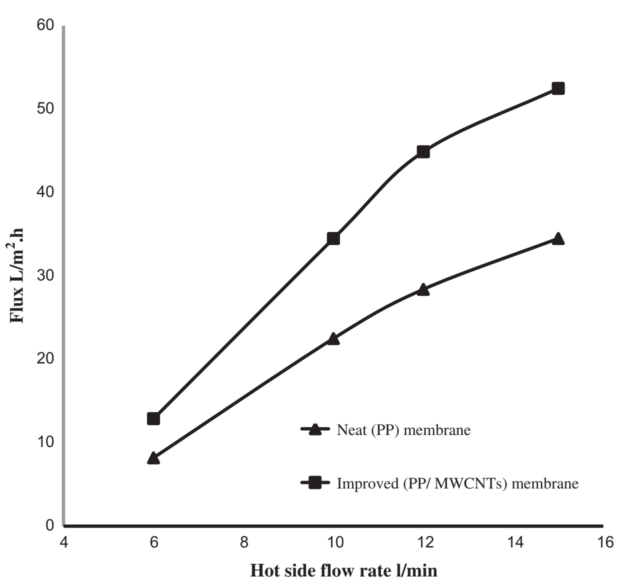

Fig. 3. Effect of feed flow rate on water flux.

3.1.3. Effect of feed TDS on flux

Fig. 4 shows the performance of the two synthesized membranes when applying four different feed water samples. The first three samples were synthesized saline water with different salt concentration 10,000, 40,000, and 100,000 mg/L, where the fourth sample was the oil field effluent water sample with salt concentration 230,000 mg/L. Fig. 4 also shows that the water flux were 19.66 and 12.43 L/m^2 h in case of using MWCNTs/PP nanocomposite membrane and neat PP membrane, respectively.

It is obvious that the MWCNTs enhanced the performance of VEDCMD with 58% at the same operating conditions [6]. The results also show that the increase in feed solute concentration results in a reduction of the VEDCMD permeate flux. This behavior is attributed to the decrease in the water vapor pressure, the driving force, with the addition of non-volatile solute in water due to the decrease in water activity in the feed [12,18].

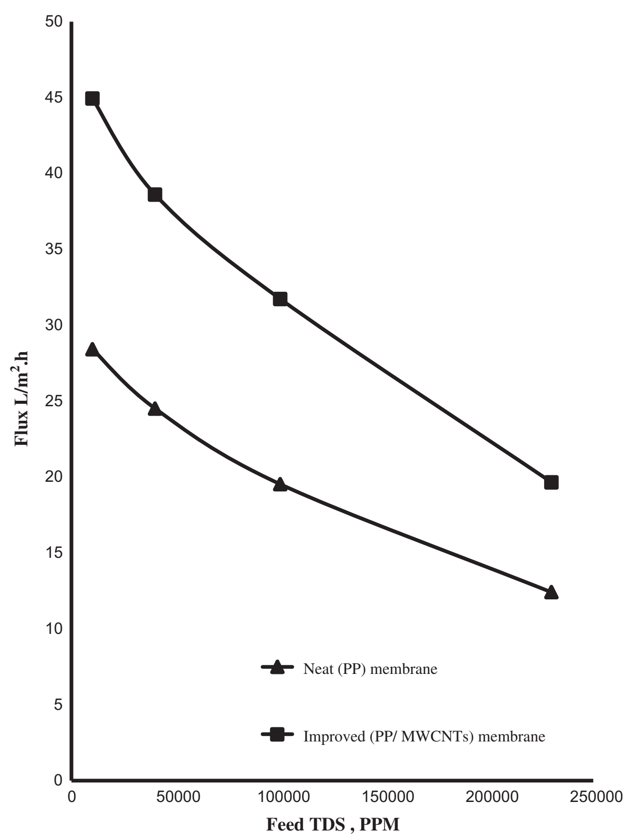

Fig. 4. Effect of feed TDS on water flux.

3.2. Effect of operating conditions on total energy consumption

3.2.1. Effect of feed temperature

Fig. 5 shows the effect of feed temperature on total energy consumption. The experiments were carried out using different feed temperatures ranging from 45 to 60˚C at hot flow rate 12 L/min, with 10,000 ppm feed TDS. As expected, total energy consumption is strongly dependent on the feed temperature, where total energy was 133.7 and 298.6 W when the feed temperatures were 45 and 60˚C, respectively, similar result was reported in [24].

3.2.2. Effect of feed flow rate

The effect of feed flow rate ranged from 6 to 15 L/min on the total energy consumed was studied at operation conditions, feed temperature 55˚C, feed TDS 10,000 ppm, as shown in Fig. 6. It can be noticed that, as the feed flow rate increases, the total energy consumed decreases. This may be due to the increase in feed flow rate that results in decrease in the temperature difference across the module (the difference between feed inlet temperature and the feed outlet temperature) which will affect the heating energy (Eq. (4)) [24]. When the feed flow rate was 6 L/min the total energy consumed was 295.1 W when compared to 155.8 W in case of 15 L/min feed flow rate.

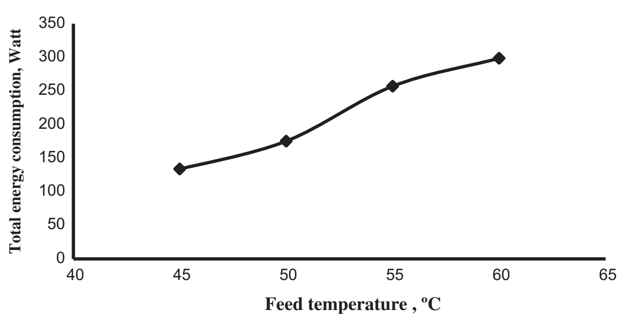

Fig. 5. Effect of feed temperature on total energy consumption.

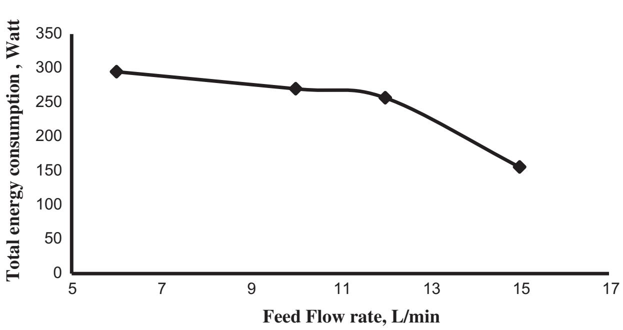

Fig. 6. Effect of feed flow rate on total energy consumption.

3.2.3. Effect of feed TDS

Fig. 7 shows the relation between the feed concentration and the total energy consumption, where different feed concentrations ranged from 10,000 to 230,000 ppm, was used at 60˚C feed temperature and feed flow rate 12 L/min. From Fig. 7, we can find that at feed concentration 10,000 mg/L the total energy consumed was 257 W, and when the feed concentration increased to 230 mg/L the total energy decreased to 148.3. These results reveal that increase in feed concentration decreases the total energy consumed which may be attributed to decrease in heating energy (Eq. (4)). Also, it should be noted that as the water salt concentration increases the heat capacity decreases which lead to decrease in heating energy.

3.3. The effect of operating conditions on SEC

3.3.1. Effect of feed temperature

Fig. 8 shows the SEC as a function of feed temperature. The experiments were carried out using different feed temperature ranging from 45 to 60˚C at hot flow rate 12 L/min, with feed TDS of 10,000 ppm. From the figure, it can be noticed that by increasing the feed temperature, for both membranes, the SEC decreased. For neat PP, the feed temperature was 45˚C, the SEC was 8,605.3 kW h/m^3, and when the feed temperature increased to 60˚C the SEC decreased to 4,207.7 kW h/m^3; while for the improved (PP/MWCNTs) at feed temperature 45˚C the SEC was 5,460.6 kW h/m^3 and when the temperature increased to 60˚C the SEC decreased to 2,999.4 kW h/m^3.

It is important to mention that, although the increase in feed temperature lead to an increase in both

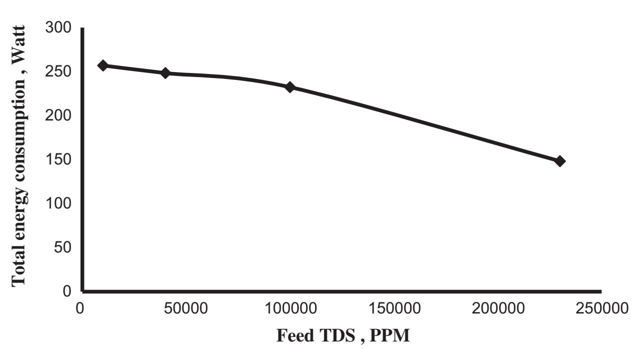

Fig. 7. Effect of feed salinity on total energy consumption.

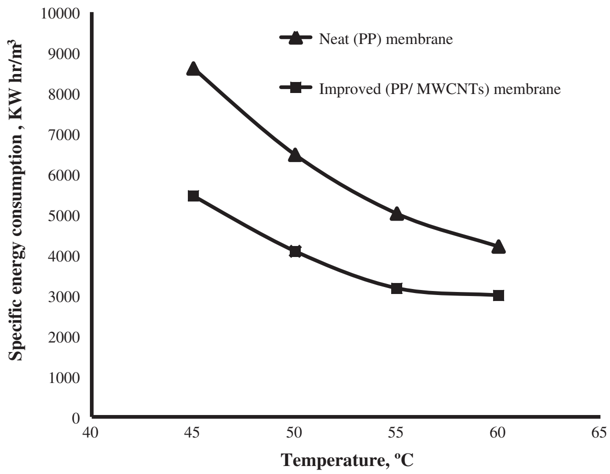

Fig. 8. Effect of hot side temperature on SEC.

thermal energy and the total energy consumed, it is found that the SEC decreased. This can be explained as follows: at high feed temperature, the heat transferred through the membrane by conduction will be negligible when compared to the heat transferred due to the mass flux [22]. Therefore, the SEC may be reduced appreciably at high operating feed temperatures [22].

3.3.2. Effect of feed flow rate

Fig. 9 shows the effect of feed flow rate ranging from 6 to 15 L/min on SEC using both the neat (PP) and improved (PP/MWCNTs) membranes, at operation conditions contained, feed temperature 55°C, feed TDS 10,000 ppm. From the figure, it can be noticed that by increasing the feed flow rate the SEC decreased. For neat PP, when the feed flow rate was 6 L/min the SEC was 19,993.4 kW h/m^3 and when the feed flow rate increased to 15 L/min the SEC decreased to 2,508.1 kW h/m^3. As for PP/MWCNTs membrane, when the feed flow rate was 6 L/min the SEC was 12,709.0 kW h/m^3, and when the feed flow rate increased to 15 L/min the SEC decreased to 1,649.2 kW h/m^3. These results agreed with the study [30], where at permeate to feed flow rate ratio was lower than unity, as current study, the SEC is inversely proportional to feed flow rate.

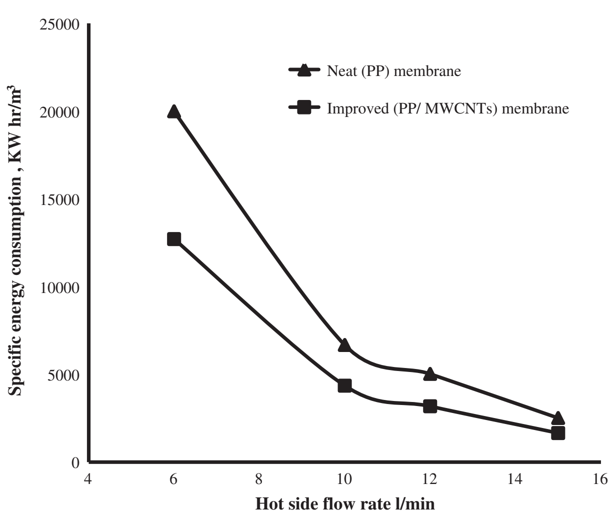

Fig. 9. Effect of feed flow rate on SEC.

3.3.3. Effect of feed TDS

Fig. 10 shows the SEC obtained for different values of the feed TDS, the experiments were tested at feed temperature 55°C, and the feed flow rate was 12 L/min. Generally, when the feed TDS increased the SEC increases due to the reduction in water flux. For neat PP, at 10,000 mg/L feed TDS the SEC was 5,022.1 kW/m^3, however, when the feed TDS increased to 230,000 mg/L (brine oil field water) the SEC increased to 6,626.4 kW h/m^3. In case of the improved MWCNT/PP membrane, at the same operating conditions, the SECs were 3,176.4 and 4,189.5 kW h/m^3 at 10,000 and 230,000 feed TDS, respectively.

3.4. The effect of operating conditions on energy efficiency

3.4.1. Effect of feed temperature

Fig. 11 shows the effect of different feed temperatures ranging from 45 to 60°C on energy efficiency.

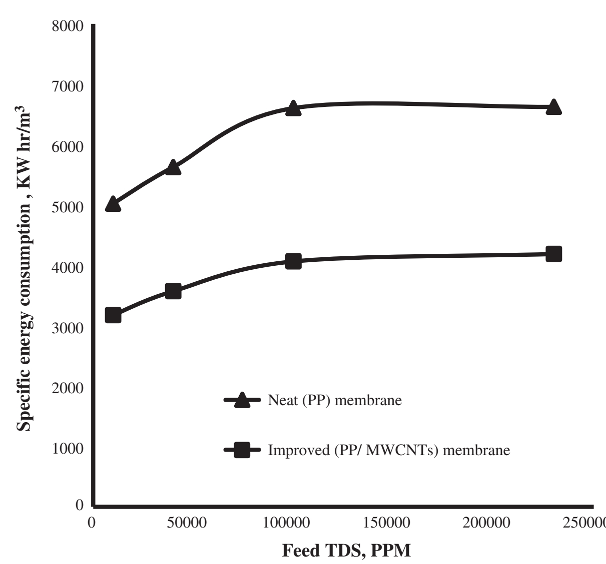

Fig. 10. Effect of feed concentration on SEC.

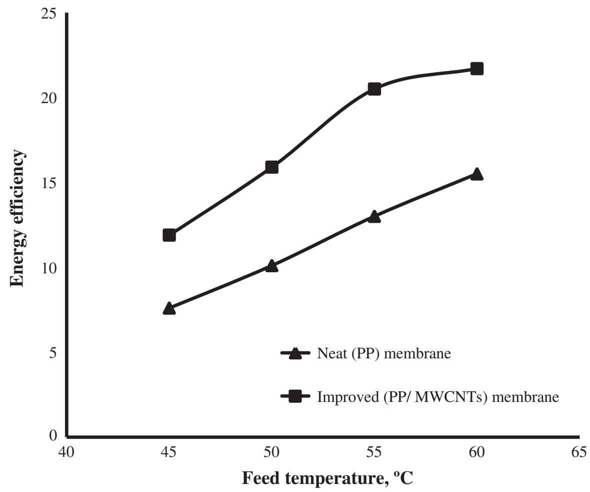

Fig. 11. Effect of feed temperature on energy efficiency.

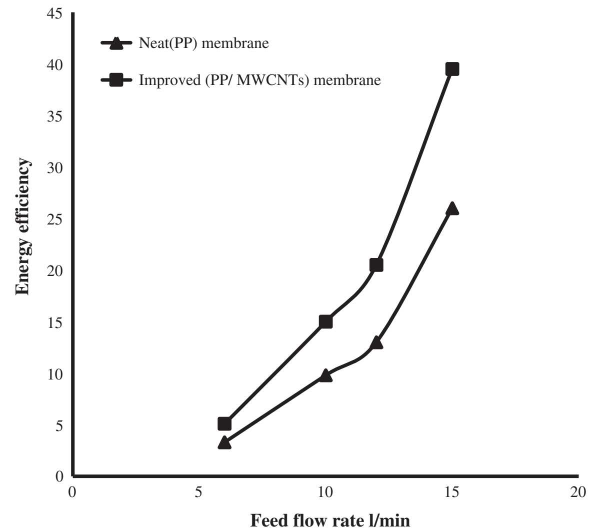

Fig. 12. Effect of feed flow rate on energy efficiency.

The experiments were tested using both membranes at hot flow rate 12 L/min, and the feed TDS was 10,000 mg/L.

For neat PP, Fig. 10 shows that when the feed temperature was 45˚C the energy efficiency was 7.6, however, when the feed temperature was 60˚C the energy efficiency increased to 15.5 due to the increase in water flux from 8.6 to 39.42 L/m^2 h. For the improved (PP/MWCNTs) membrane at the same operating conditions, it can be found that at the feed temperature 45˚C the energy efficiency was 11.9, and when the feed temperature increased to 60˚C the energy efficiency increased to 21.7 due to the increase in water flux from 13.6 to 55.3 L/m^2 h. These results are supported by previous studies [5,31,32] where they found that when VEDCMD system is operated at high feed temperature, high energy efficiency is anticipated.

3.4.2. Effect of feed flow rate

Effect of feed flow rate on the energy efficiency for both membranes was studied as shown in Fig. 12. The experiments were tested at hot side temperature 55˚C with TDS 10,000 mg/L. The results show that the increase in the feed flow rate from 6 to 15 L/min increases the energy efficiency from 3.3 to 26 in case of neat PP membrane; however, when the improved (PP/MWCNTs) membrane was used the energy efficiency increased from 5.1 to 39.5 [5,31,32].

3.4.3. Effect of feed concentration

Fig. 13 shows the energy efficiency obtained for different values of the feed TDS, for both membranes

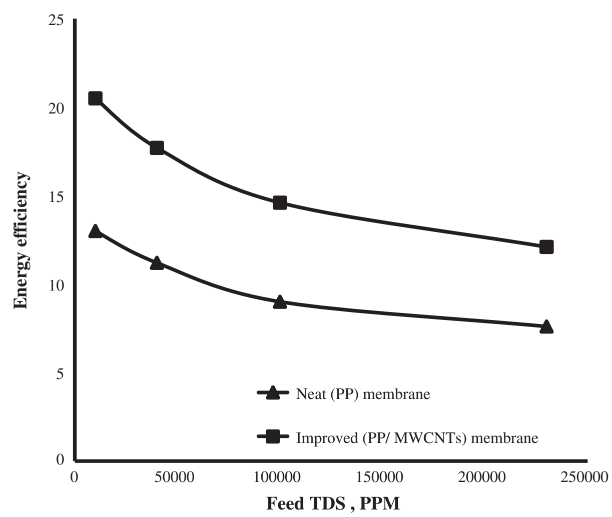

Fig. 13. Effect of feed concentration on energy efficiency.

at hot side temperature 55˚C, and the feed flow rate was 12 L/min. It can be found from Fig. 13 that when the feed TDS was 10,000 mg/L the energy efficiency was 13.0, and when the feed TDS increased to 230,000 mg/L the flux decreased to 12.43 L/m^2 h with a decrease in energy efficiency to 7.6. When improved (PP/MWCNTs) membrane was used at the same operating condition, at feed TDS 10,000 mg/L the energy efficiency was 20.5; however, when the feed TDS increased to 230,000 mg/L with a slight increase in the energy efficiency it decreased to 12.1.

Table 3.
Comparison between the current study and previous DCMD studies

References	EC (kW h/m^3)	Energy efficiency	Feed TDS
[24]	4,580	–	Distillate water
[5]	–	34	600 ppm glucose
[31]	–	4.1	Sea water
[32]	–	1.38	30,000 ppm
Current study	3,176.4	20.5	10,000 ppm
	3,573.5	17.7	40,000 ppm
	4,067.0	14.6	100,000 ppm
	4,189.5	12.1	230,000 ppm

3.5. Comparisons between previous work and current study

In this section, we shed light on our status by comparing the performance of our prepared membranes and that of the available previous works in terms of energy efficiency (η_E) and SEC via DCMD process using different feed concentrations, as shown in Table 3.

It is clear that the current study has better performance with higher permeate flux and enhanced energy efficiency (η_E) with lower SEC. This can be due to the characteristic of the prepared membrane that enhance the performance and increased the permeate flux, energy efficiency (η_E) and decreasing the SEC. Also, it may be due to the modification of DCMD system configuration using vacuum enhancement, i.e. VEDCMD system configuration.

4. Conclusions

The VEDCMD performance of both neat PP and improved PP MWCNT/polypropylene membranes was studied at different operation conditions such as different feed temperatures, different flow rates, and different salt concentrations. In this work, the calculations of SEC, energy efficiency (η_E), and the comparison between the two used membranes were achieved. The results showed that the improved (PP/MWCNTs) membrane is achieving better performance than the neat (PP) membrane in membrane distillation processes and gave higher permeate flux and energy efficiency (η_E) with lower SEC at the same operating conditions.

Also, the current study reveals that our prepared membranes have better performance than the available previous works. It obtained higher permeate flux and enhanced energy efficiency (η_E) with lower SEC.

Acknowledgements

It is a pleasure to acknowledge the financial support provided by the Science and Technological Development Fund (STDF) in Egypt through Grant 5240 (Egyptian Desalination Research Center of Excellence, EDRC).

References

[1] M. Khayet, T. Matsuura, Membrane Distillation: Principles and Applications, Elsevier, Amsterdam, 2011.
[2] M. Schorr, Desalination Trends and Technologies, InTech, Rijeka, 2011.
[3] K.W. Lawson, D.R. Lloyd, Membrane distillation, J. Membr. Sci. 124(1) (1997) 1–25.
[4] P. Wang, T. Chung, Recent advances in membrane distillation processes: Membrane development, configuration design and application exploring, J. Membr. Sci. 474 (2015) 39–56.
[5] V.A. Bui, L.T.T. Vu, M.H. Nguyen, Simulation and optimisation of direct contact membrane distillation for energy efficiency, Desalination 259 (2010) 29–37.
[6] T.L.S. Silva, S. Morales-Torres, J.L. Figueiredo, A.M.T. Silva, Multi-walled carbon nanotube/PVDF blended membranes with sponge- and finger-like pores for direct contact membrane distillation, Desalination 357 (2015) 233–245.
[7] M.M.A. Shirazi, A. Kargari, M. Tabatabaei, Evaluation of commercial PTFE membranes in desalination by direct contact membrane distillation, Chem. Eng. Process. 76 (2014) 16–25.
[8] Y.M. Manawi, M.A.M.M. Khraisheh, A.K. Fard, F. Benyahia, S. Adham, A predictive model for the assessment of the temperature polarization effect in direct contact membrane distillation desalination of high salinity feed, Desalination 341 (2014) 38–49.
[9] M.M.A. Shirazi, A. Kargari, M.J.A. Shirazi, Direct contact membrane distillation for seawater desalination, Desalin. Water Treat. 49(1–3) (2012) 368–375.
[10] T.-C. Chen, C.-D. Ho, H.-M. Yeh, Theoretical modeling and experimental analysis of direct contact membrane distillation, J. Membr. Sci. 330(1–2) (2009) 279–287.
[11] T.Y. Cath, V.D. Adams, A.E. Childress, Vacuum enhanced direct contact membrane distillation, US Patent No. 7,608,188 B2 (2009).
[12] C.R. Martinetti, A.E. Childress, T.Y. Cath, High recovery of concentrated RO brines using forward osmosis and membrane distillation, J. Membr. Sci. 331 (2009) 31–39.
[13] J. Zhang, J.-D. Li, M. Duke, Z. Xie, S. Gray, Performance of asymmetric hollow fibre membranes in membrane distillation under various configurations and vacuum enhancement, J. Membr. Sci. 362 (2010) 517–528.
[14] D. Hou, J. Wang, D. Qu, Z. Luan, X. Ren, Fabrication and characterization of hydrophobic PVDF hollow fiber membranes for desalination through direct contact membrane distillation, Sep. Purif. Technol. 69 (2009) 78–86.

[15] L. García-Fernández, M.C. García-Payo, M. Khayet, Effects of mixed solvents on the structural morphology and membrane distillation performance of PVDF-HFP hollow fiber membranes, J. Membr. Sci. 468 (2014) 324–338.
[16] Ó. Andrjesdóttir, C.L. Ong, M. Nabavi, S. Paredes, A.S.G. Khalil, B. Michel, D. Poulikakos, An experimentally optimized model for heat and mass transfer in direct contact membrane distillation, Int. J. Heat Mass Transfer 66 (2013) 855–867.
[17] J. Woods, J. Pellegrino, J. Burch, Generalized guidance for considering pore-size distribution in membrane distillation, J. Membr. Sci. 368 (2011) 124–133.
[18] H.J. Hwang, K. He, S. Gray, J. Zhang, I.S.Moon, Direct contact membrane distillation (DCMD): Experimental study on the commercial PTFE membrane and modeling, J. Membr. Sci. 371 (2011) 90–98.
[19] M. Gryta, Effectiveness of water desalination by membrane distillation process, Membranes 2 (2012) 415–429.
[20] L. Martínez, J.M. Rodríguez-Maroto, Effects of membrane and module design improvements on flux in direct contact membrane distillation, Desalination 205 (2007) 97–103.
[21] M. Khayet, Membranes and theoretical modeling of membrane distillation: A review, Adv. Colloid Interface Sci. 164 (2011) 56–88.
[22] M. Khayet, Solar desalination by membrane distillation: Dispersion in energy consumption analysis and water production costs (a review), Desalination 308 (2013) 89–101.
[23] E.K. Summers, H.A. Arafat, J.H. Lienhard V, Energy efficiency comparison of single-stage membrane distillation (MD) desalination cycles in different configurations, Desalination 290 (2012) 54–66.
[24] A. Criscuoli, M.C. Carnevale, E. Drioli, Evaluation of energy requirements in membrane distillation, Chem. Eng. Process. 47 (2008) 1098–1105.
[25] E. Drioli, A. Ali, F. Macedonio, Membrane distillation: Recent developments and perspectives, Desalination 356 (2015) 56–84.
[26] K. Okiel, A.H.M. El-Aassar, T. Temraz, S. El-Etriby, H.A. Shawky, Performance assessment of synthesized CNT/polypropylene composite membrane distillation for oil field produced water desalination, Desalin. Water Treat. (2015) 1–13.
[27] I.J. Karassik, J.P. Messina, P. Cooper, C.C. Heald, Pump Hand Book, McGraw-Hill, New York, NY, 2008.
[28] H. Sun, R. Feistel, M. Koch, A. Markoe, New equations for density, entropy, heat capacity, and potential temperature of a saline thermal fluid, Deep Sea Res. Part I 55(10) (2008) 1304–1310.
[29] M.H. Sharqawy, J.H. Lienhard V, S.M. Zubair, Thermophysical properties of seawater: A review of existing correlations and data, Desalin. Water Treat. 16 (2010) 354–380.
[30] S. Lin, N.Y. Yip, M. Elimelech, Direct contact membrane distillation with heat recovery: Thermodynamic insights from module scale modeling, J. Membr. Sci. 453 (2014) 498–515.
[31] H. Lee, F. He, L. Song, J. Gilron, K.K. Sirkar, Desalination with a cascade of cross-flow hollow fiber membrane distillation devices integrated with a heat exchanger, AICHE J. 57 (2011) 1780–1795.
[32] G. Zuo, R. Wang, R. Field, A.G. Fane, Energy efficiency evaluation and economic analyses of direct contact membrane distillation system using Aspen Plus, Desalination 283 (2011) 237–244.